

Lessons in Multi-site DTI Acquisition- the BIRN experience

Randy L. Gollub, MD, PhD

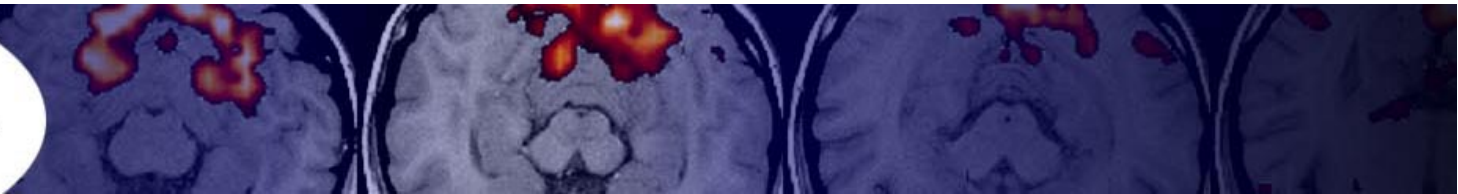
Massachusetts General Hospital

Departments of Psychiatry & Radiology

41st Annual meeting of the Society for Neuroscience
Washington, DC
November 11, 2011

Acknowledgements

- Morphometry BIRN
 - Susumu Mori
 - Allen Song
 - Jorge Jovicich
 - Karl Helmer
- Carlo Pierpoli (External Advisor to NAMIC)
- Tonya White and the Mind Research Network Clinical Imaging Consortium team



Morphometry BIRN: DTI acquisition

See:

https://xwiki.nbirn.org:8443/bin/view/Morphometry-BIRN/mBIRN_DTI_protocols

BIRN Sites and Collaborators

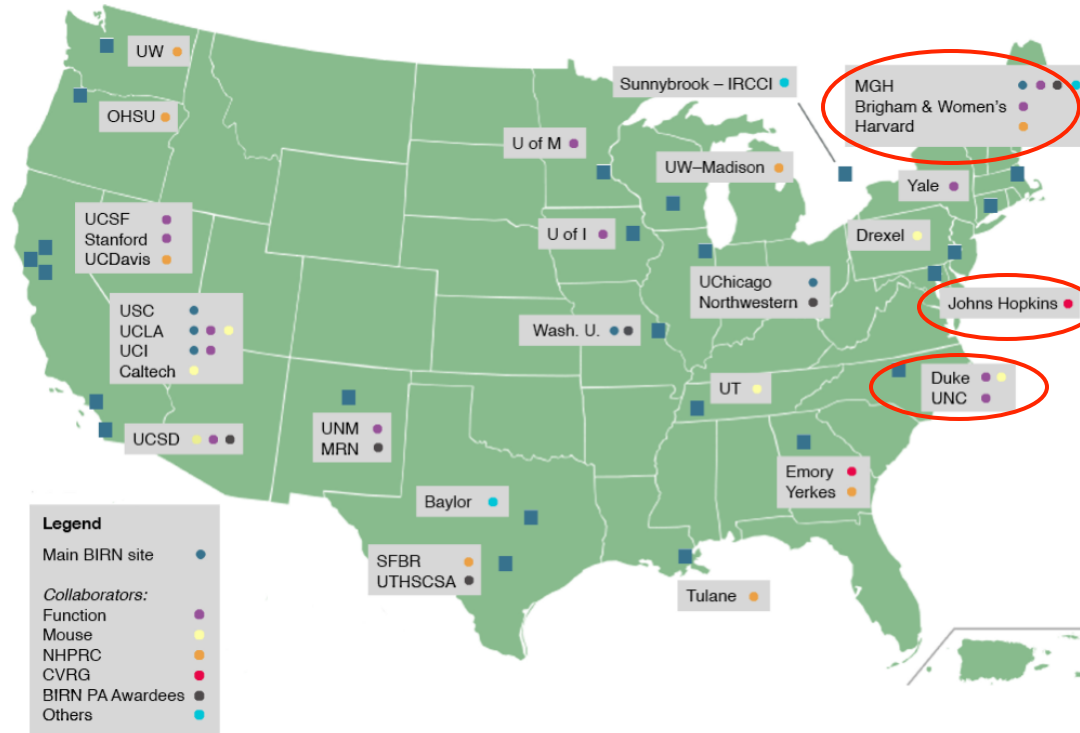


Image Data Repository

The screenshot shows a web browser window displaying the XNAT Image Data Repository. The browser's address bar shows the URL <https://central.xnat.org/>. The page features a navigation menu with 'Home' and 'Tools' options. A search bar is present with a 'Search' button and a 'Guest (Login) (Register)' link. A sidebar on the left contains a 'Launch Uploader' button and a tree view of project categories: 'Projects' (with sub-items 'Recent', 'Favorite', 'My projects', 'Other projects'), 'Stored Searches', and 'Data'. The main content area is titled 'Search' and indicates that the repository currently contains 227 Projects, 3181 Subjects, and 4382 Imaging Sessions. Below this is a search form with tabs for 'Projects', 'Subjects', 'MR', 'PET', and 'CT'. The form includes input fields for 'ID', 'Name', 'Description', 'Keywords', and 'Investigator', along with a 'Submit' button. A 'Recent Data Activity' table is also visible, showing a single entry: ADHD200, MR, 1, NEW. The footer of the page includes the text 'powered by XNAT' and a 'Done' status indicator.

CENTRAL

xnat.org <https://central.xnat.org/> xnat central

Most Visited MIT Yoga 24X7: Home Relationship between... Research Computing LHS portal Extended cortical act... Sex Differences in th... MyNutrikids Microstructure of Fr... >>

CENTRAL +

XNAT

Guest (Login) (Register) Search Advanced

Home Tools

Search

CENTRAL currently contains 227 Projects, 3181 Subjects, and 4382 Imaging Sessions.

Projects Subjects MR PET CT

ID Name Description

Keywords Investigator

Submit

Projects

mBIRN_calib
Project ID: Calib PI: Karl Helmer
This data set consists of spoiled gradient-recalled echo magnetic resonance imaging data from five healthy volunteers (four males and one female) scanned t ...
[Request access](#) to this project.

Oasis Cross-Sectional Studies
Project ID: CENTRAL_OASIS_CS PI: Dan Marcus
See www.oasis-brains.org for details.
[Request access](#) to this project.

PALS: Population-Average, Landmark- and Surface-based atlas
Project ID: PALS
Cases composing the PALS atlas as borrowed from the OASIS cross-sectional data set. Includes raw T1 images, FSL's FAST tissue-segmented images, and Freesurfe ...
[Request access](#) to this project.

Sample DICOM dataset
Project ID: Sample_DICOM
[Request access](#) to this project.

Recent Data Activity

ADHD200	MR	1	NEW
---------	----	---	-----

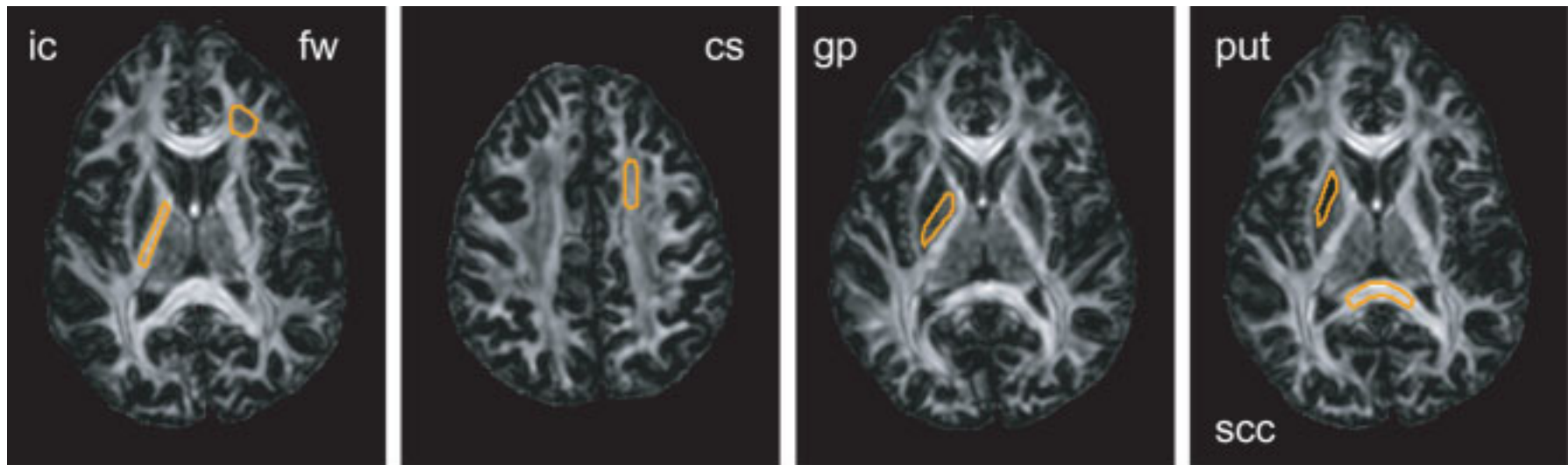
Done

powered by **XNAT**

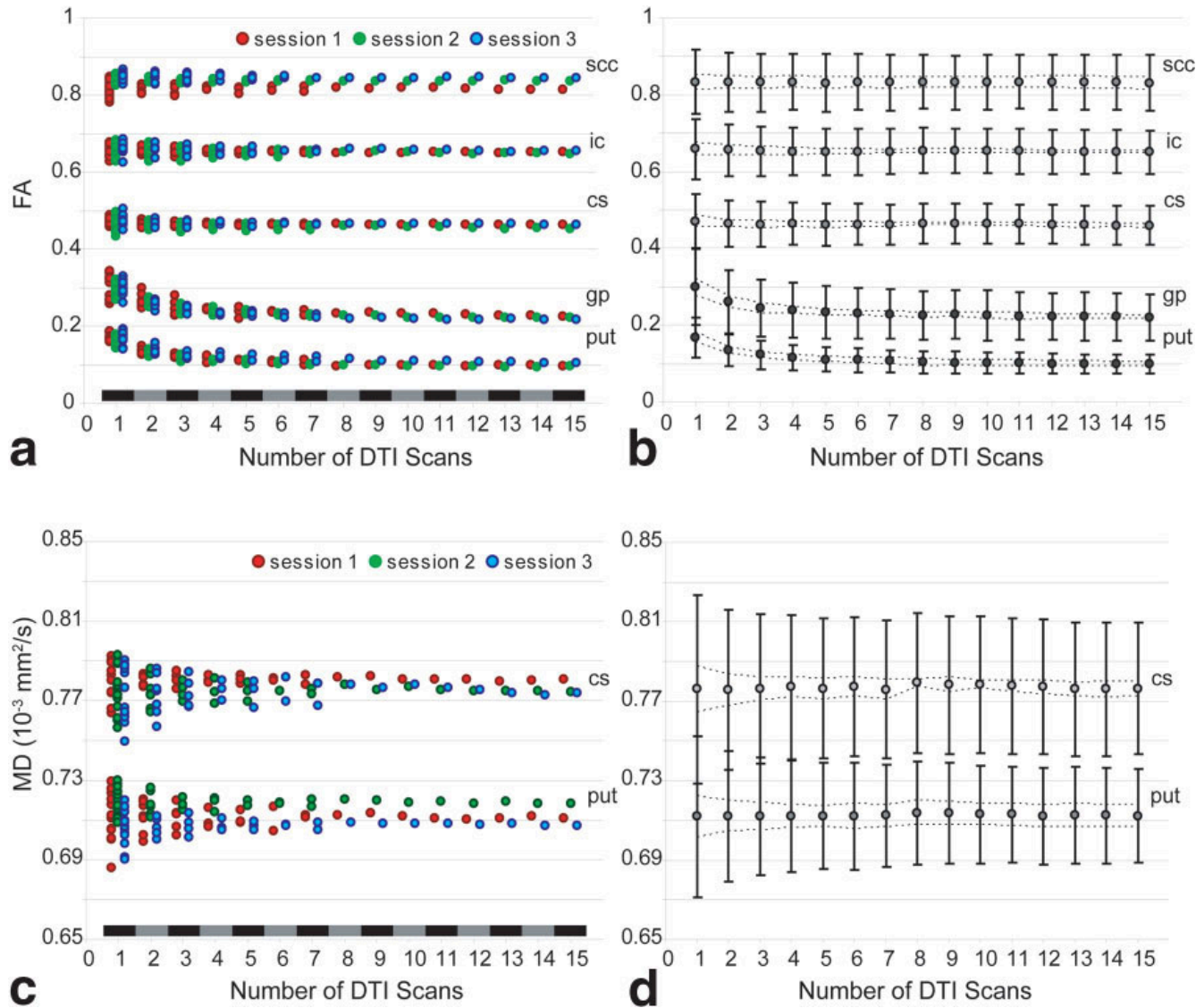
Effects of Signal-to-Noise Ratio on the Accuracy and Reproducibility of Diffusion Tensor Imaging-Derived Fractional Anisotropy, Mean Diffusivity, and Principal Eigenvector Measurements at 1.5T

Jonathan A.D. Farrell, BS,¹⁻³ Bennett A. Landman, MEng,⁴ Craig K. Jones, PhD,^{1,2}
Seth A. Smith, PhD,^{1,2} Jerry L. Prince, PhD,^{2,4,5} Peter C.M. van Zijl, PhD,¹⁻³
Susumu Mori, PhD^{1,2,4*}

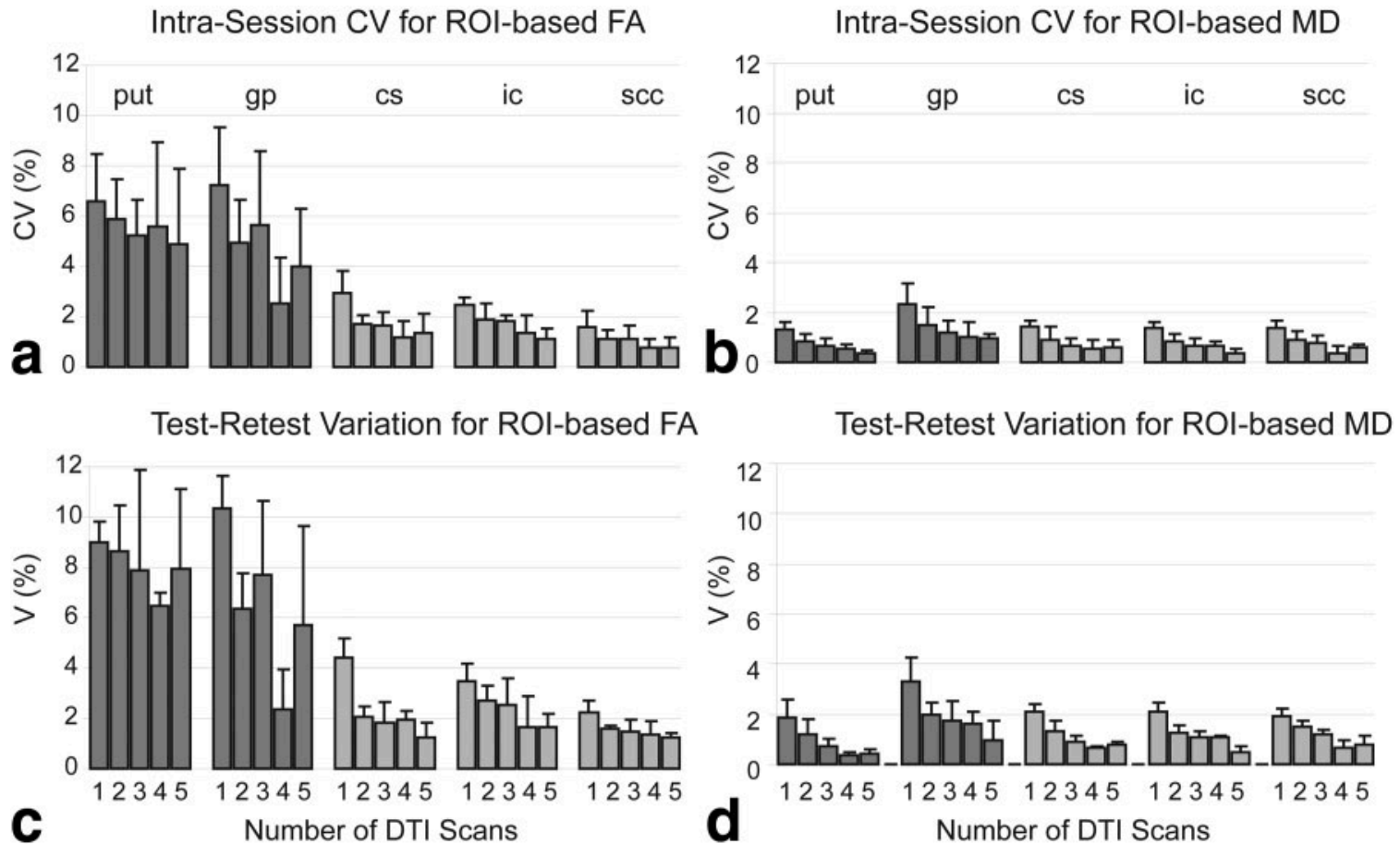
JOURNAL OF MAGNETIC RESONANCE IMAGING 26:756-767 (2007)



Optimal DTI scan parameters are dictated by the ROI



Optimal DTI scan parameters produce reliable results within and across sessions

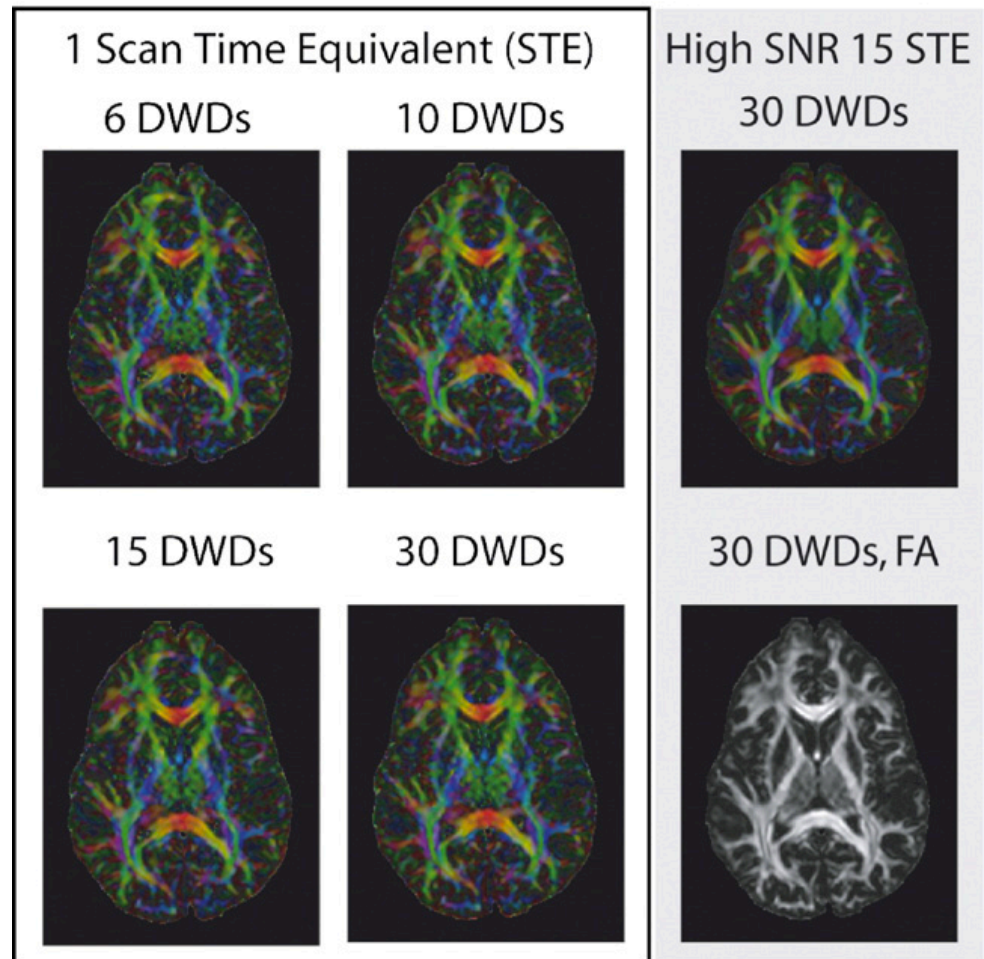


Effects of diffusion weighting schemes on the reproducibility of DTI-derived fractional anisotropy, mean diffusivity, and principal eigenvector measurements at 1.5T

Bennett A. Landman,^a Jonathan A.D. Farrell,^{b,c,d} Craig K. Jones,^{b,c} Seth A. Smith,^{b,c} Jerry L. Prince,^{a,b,e} and Susumu Mori^{a,b,c,*}

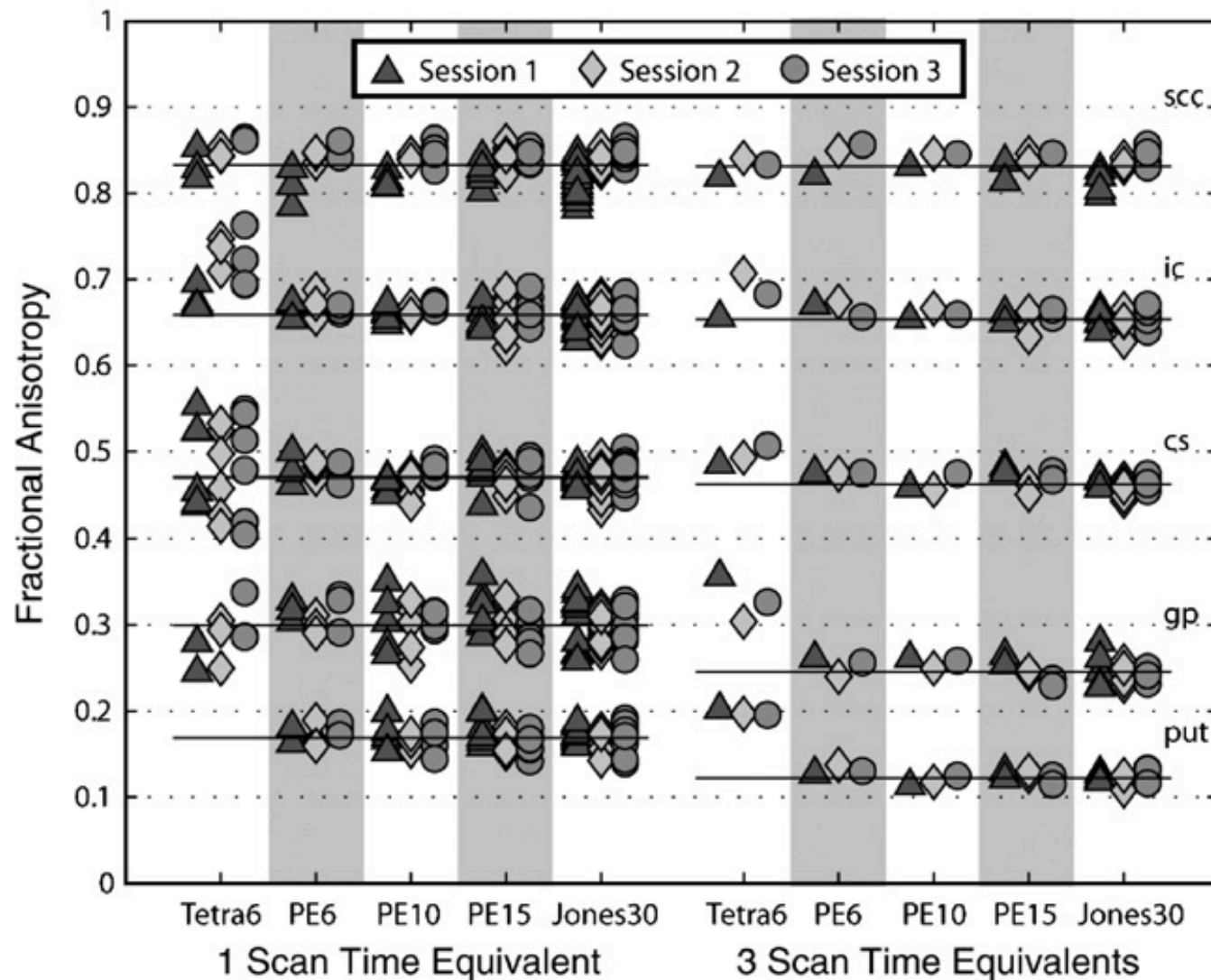
Diffusion Tensor Colormap Images

Differences in DTI contrasts due to different DW schemes are small relative to intra-session variability.



Well balanced DW schemes give comparable results across sessions

Mean FA in Region of Interest



DTI processing steps that have to be matched across sites or performed at a central site

DTI Data transfer - storage – tracking
Initial quality control

Processing pipeline:

Importing data and transforming to common format

Motion and eddy-current distortion correction

Registration to template

EPI distortion correction

Rotation of b-matrices

Production of “corrected” raw images (interpolation)

Tensor computation (correct weighting)

Robust tensor estimation

Computation of tensor derived variables

Production of tensor data in stereotaxic space

Upload of processed data into shared database

Examples of commonly occurring DWI acquisition problems

- incomplete dataset
- incorrect slice thickness
- incorrect in plane resolution
- incorrect gap between slices
- subject motion
- cardiac pulsation
- EPI ghosting
- image acquisitions have different starting location
- spurious labels in background
- insufficient brain coverage
- b matrix problems
- replicates averaged

Comprehensive Approach for Correction of Motion and Distortion in Diffusion-Weighted MRI

G.K. Rohde,^{1,3*} A.S. Barnett,² P.J. Basser,¹ S. Marenco,² and C. Pierpaoli¹

Patient motion and image distortion induced by eddy currents cause artifacts in maps of diffusion parameters computed from diffusion-weighted (DW) images. A novel and comprehensive approach to correct for spatial misalignment of DW imaging (DWI) volumes acquired with different strengths and orientations of the diffusion sensitizing gradients is presented. This approach uses a mutual information-based registration technique and a spatial transformation model containing parameters that correct for eddy current-induced image distortion and rigid body motion in three dimensions. All parameters are optimized simultaneously for an accurate and fast solution to the registration problem. The images can also be registered to a normalized template with a single interpolation step without additional computational cost. Following registration, the signal amplitude of each DWI volume is corrected to account for size variations of the object produced by the distortion correction, and the *b*-matrices are properly recalculated to account for any rotation applied during registration. Both qualitative and quantitative results show that this approach produces a significant improvement of diffusion tensor imaging (DTI) data acquired in the human brain. Magn Reson Med 51:103–114, 2004. Published 2003 Wiley-Liss, Inc.†

Key words: image registration; mutual information; distortion correction; motion correction; eddy currents

reduce residual eddy current-induced distortions in DW images are based on either field maps or images.

In a field map-based correction scheme, such as that presented by Jezzard et al. (8), one measures the magnetic field produced by the eddy currents and then corrects the distortion using the field map and theoretical models of how field inhomogeneities distort the images. The major obstacle to implementation is the difficulty of rapidly acquiring reliable field maps.

In an image-based registration scheme, one uses a cost function *Q* to measure how well the images are spatially aligned. First, a target image is chosen as a reference for all other images in the data set (source images). Because it is usually less distorted and has a higher signal-to-noise ratio (SNR) than the heavily DW images, the image acquired with no diffusion sensitization (the T_2 -weighted image), is usually used as the target image for registering DW images. Next, using a spatial transformation model, one aligns all other images to the target image by optimizing a cost function. Image-based registration schemes differ from each other in terms of 1) the definition of *Q*, 2) the types of transformations applied to the image in searching for the



ELSEVIER

NeuroImage

www.elsevier.com/locate/ynimg
NeuroImage 26 (2005) 673–684

Estimating intensity variance due to noise in registered images: Applications to diffusion tensor MRI

Gustavo K. Rohde,^{a,b,*} Alan S. Barnett,^c Peter J. Basser,^a and Carlo Pierpaoli^a

^a*STBB/LIMB/NICHD, National Institutes of Health, Building 13, Room 3w16, 13 South Drive, Bethesda, MD 20892, USA*

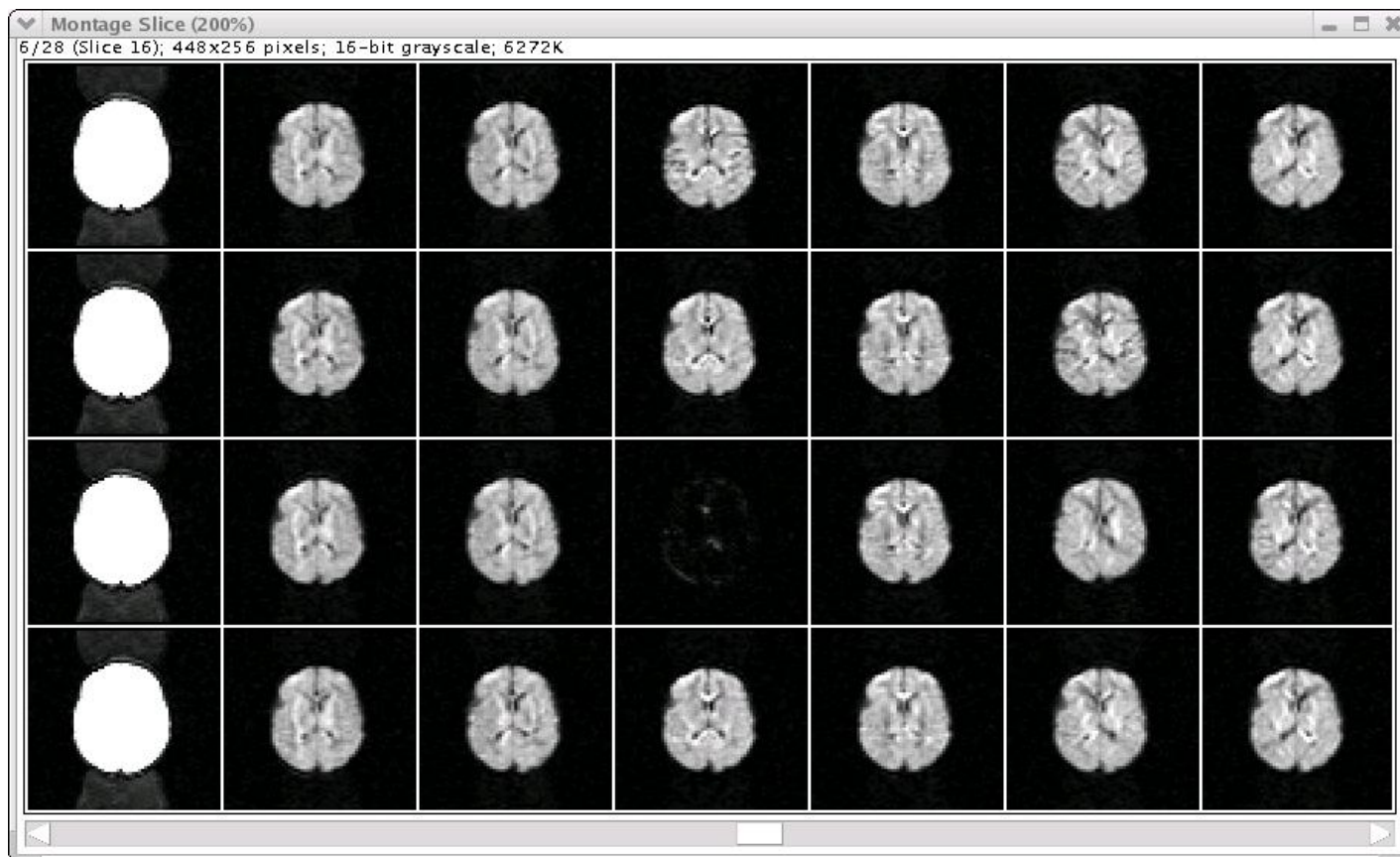
^b*Applied Mathematics and Scientific Computation Program, University of Maryland, College Park, MD 20742, USA*

^c*NIMH, National Institutes of Health, Bethesda, MD 20892, USA*

Received 14 May 2004; revised 7 February 2005; accepted 17 February 2005

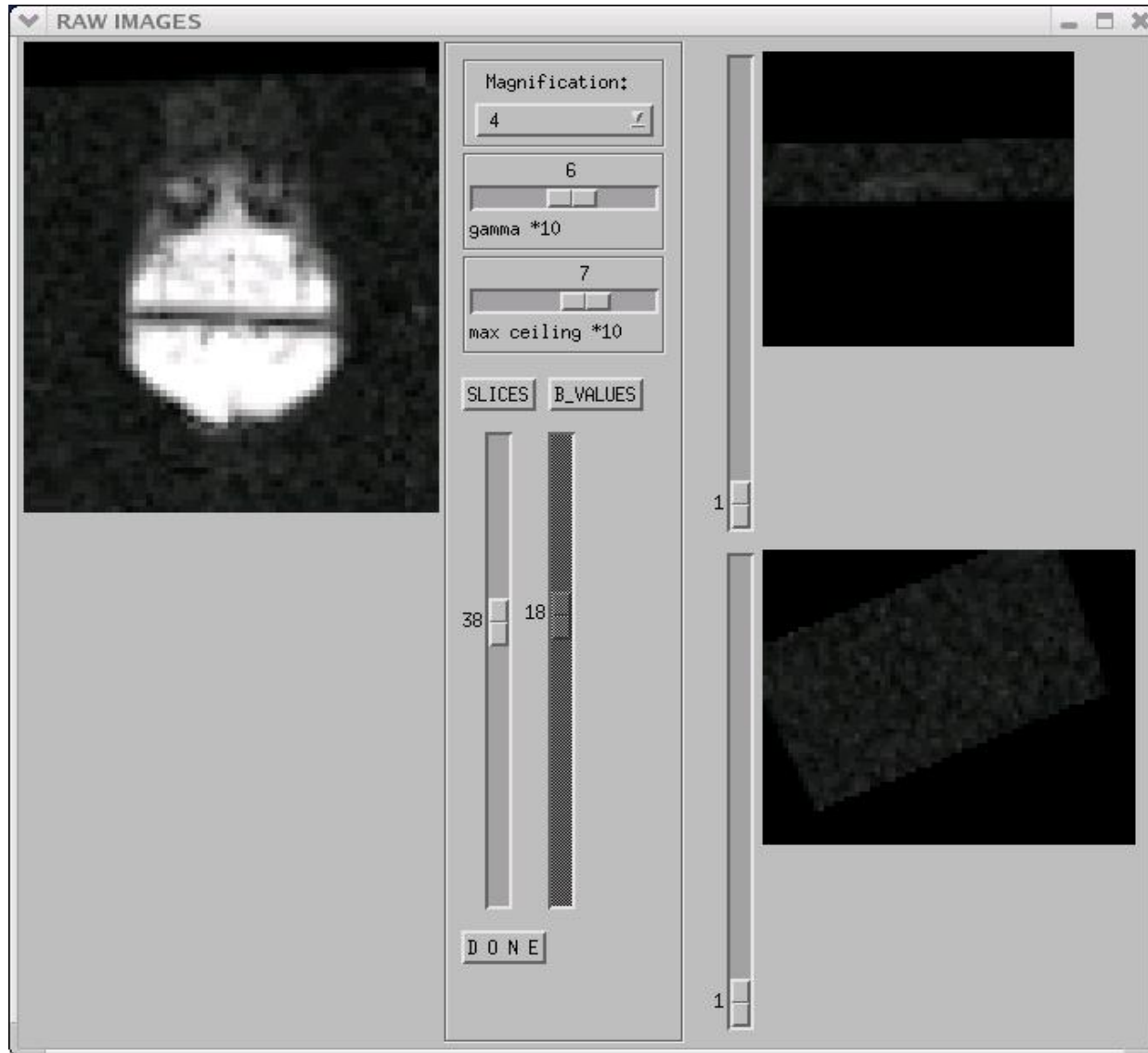
Available online 7 April 2005

Data set with a corrupted image



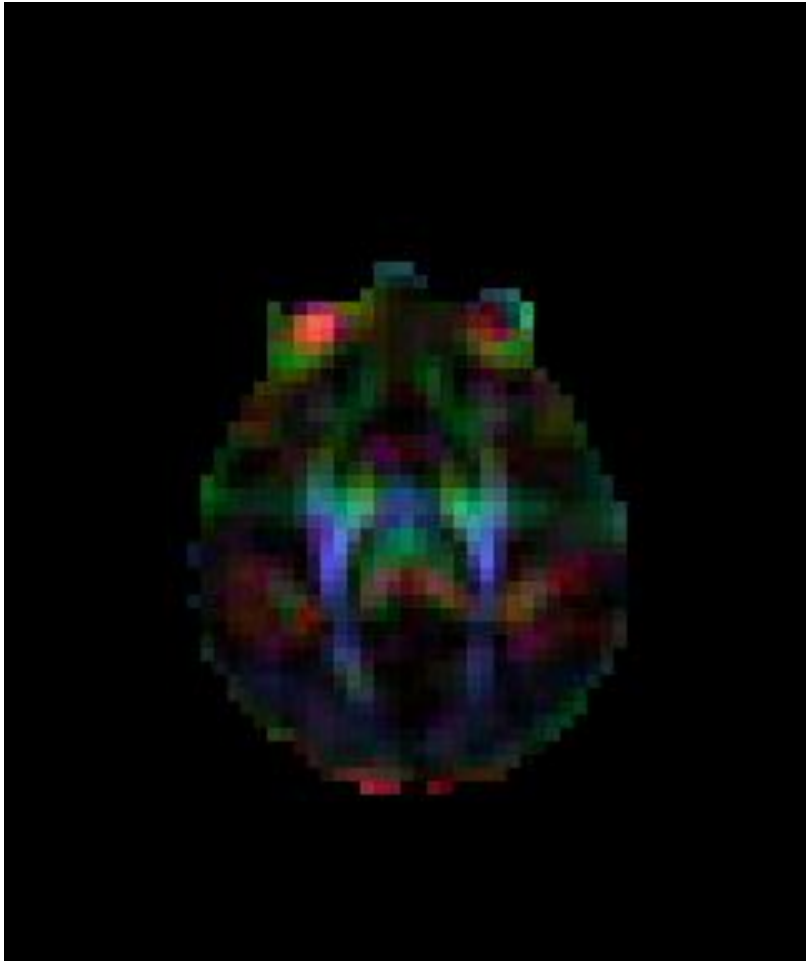
Unpublished presentation from Carlo Pierpoli, 2007

Artifact after registration

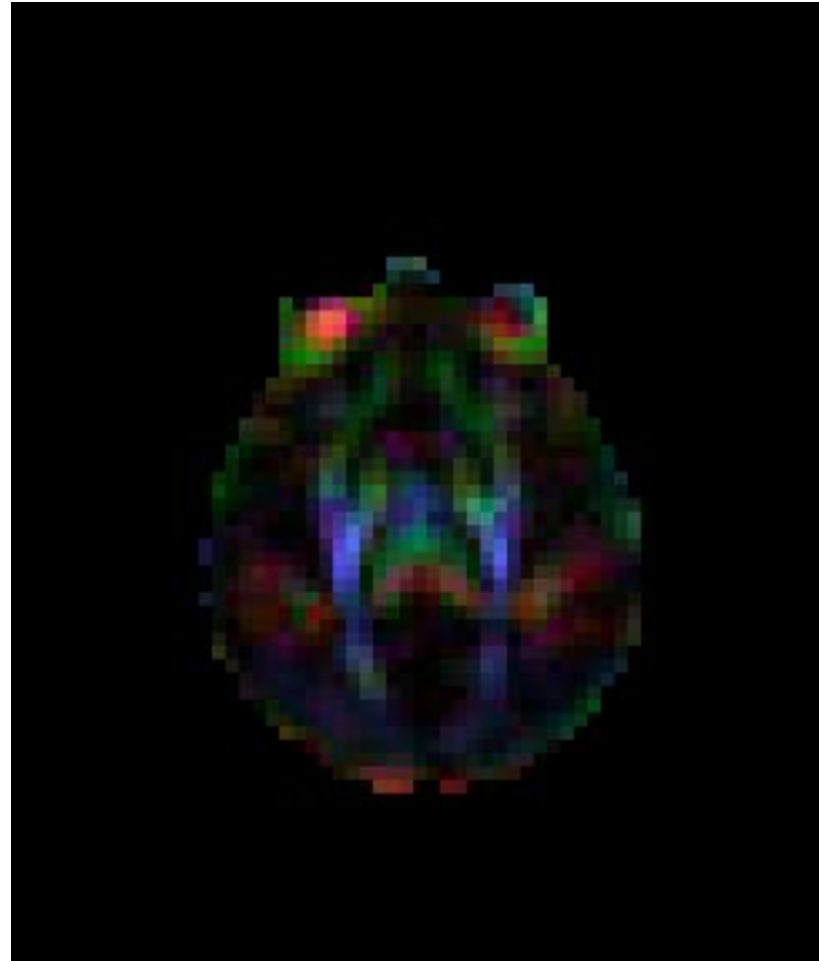


Unpublished presentation from Carlo Pierpoli, 2007

DEC MAP



Conventional tensor fitting



Robust tensor fitting using RESTORE

Unpublished presentation from Carlo Pierpoli, 2007

RESTORE: Robust Estimation of Tensors by Outlier Rejection

Lin-Ching Chang,¹ Derek K. Jones,^{1,2} and Carlo Pierpaoli^{1*}

Signal variability in diffusion weighted imaging (DWI) is influenced by both thermal noise and spatially and temporally varying artifacts such as subject motion and cardiac pulsation. In this paper, the effects of DWI artifacts on estimated tensor values, such as trace and fractional anisotropy, are analyzed using Monte Carlo simulations. A novel approach for robust diffusion tensor estimation, called RESTORE (for robust estimation of tensors by outlier rejection), is proposed. This method uses iteratively reweighted least-squares regression to identify potential outliers and subsequently exclude them. Results from both simulated and clinical diffusion data sets indicate that the RESTORE method improves tensor estimation compared to the commonly used linear and nonlinear least-squares tensor fitting methods and a recently proposed method based on the Geman–McClure M-estimator. The RESTORE method could potentially remove the need for cardiac gating in DWI acquisitions and should be applicable to other MR imaging techniques that use univariate or multivariate regression to fit MRI data to a model. Magn Reson Med 53:1088–1095, 2005. Published 2005 Wiley-Liss, Inc.[†]

Key words: robust estimation; outliers; trace; anisotropy; diffusion; tensor

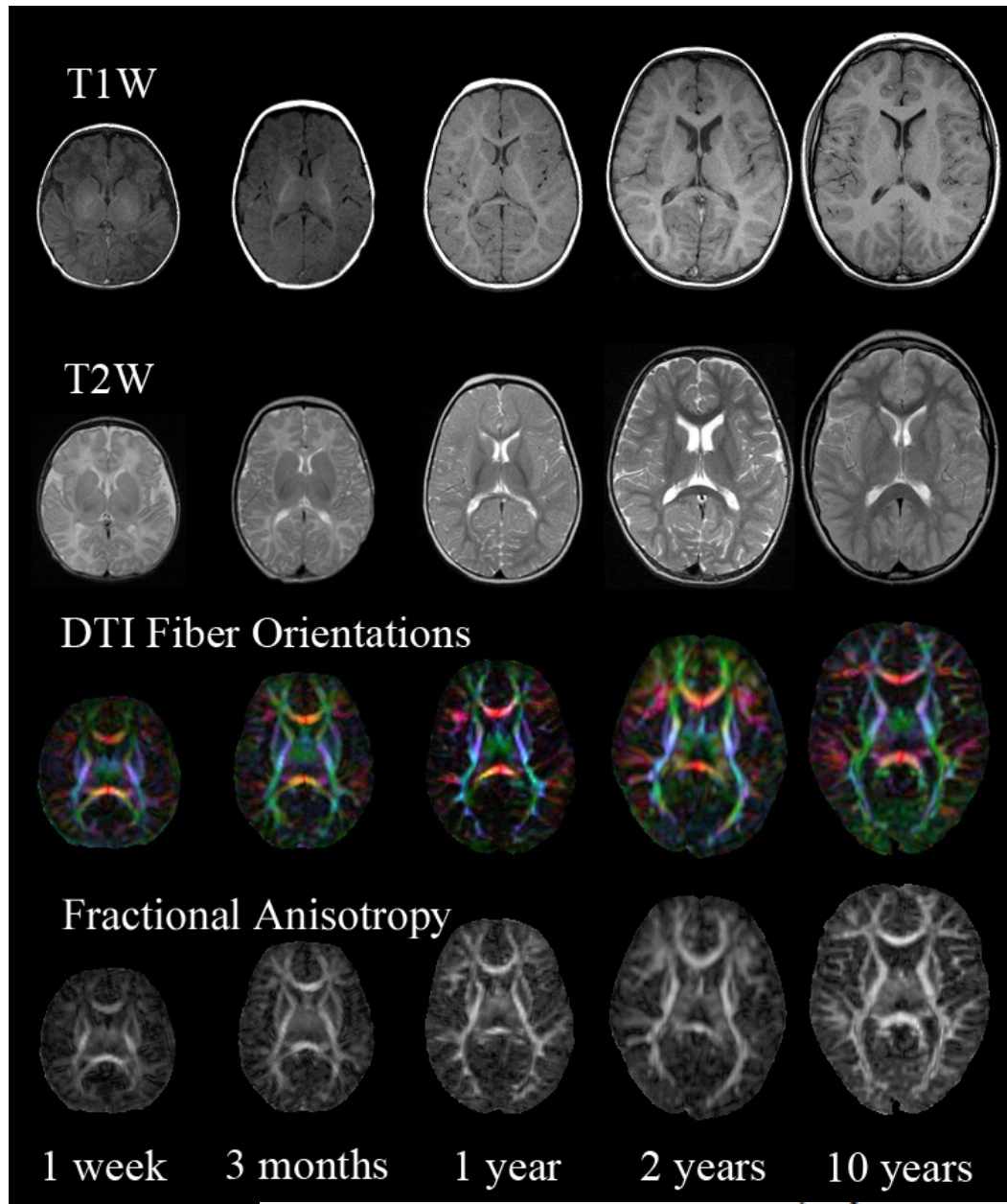
not account for signal perturbations and potential outliers that originate from artifacts. While the signal variability produced by thermal noise is approximately Gaussian distributed (3), signal variability produced by physiologic noise and other artifacts does not have a known parametric distribution and currently cannot be modeled. Situations in which experimental errors do not follow a Gaussian distribution, or are unknown, are generally addressed statistically by using “robust” estimators, which are less sensitive to the presence of outliers.

Surprisingly, the use of robust estimators has been largely neglected by the DT-MRI community. We are aware of only one robust tensor estimation approach recently proposed by Mangin et al. (4), which is based on the well-known Geman-McClure M-estimator (5) (we will refer to Mangin’s approach as GMM in this paper). This approach uses an iteratively reweighted least-squares fitting in which the weight of each data point is set to a function of the residuals of the previous iteration. The GMM method ensures that potentially artifactual data points having large residuals are given lower weights in

NIH MRI Study of Normal Brain Development

Public Website:
<http://www.brain-child.org/>

Unpublished
presentation by
Carlo Pierpoli, 2007



Lessons learned

No matter how carefully the study is planned expect relatively large variability in the quality of the acquired data

Run a pilot study with all the sites involved prior to starting data collection

Use strict quality control criteria

Set up a robust data processing pipeline to reduce variability across sites



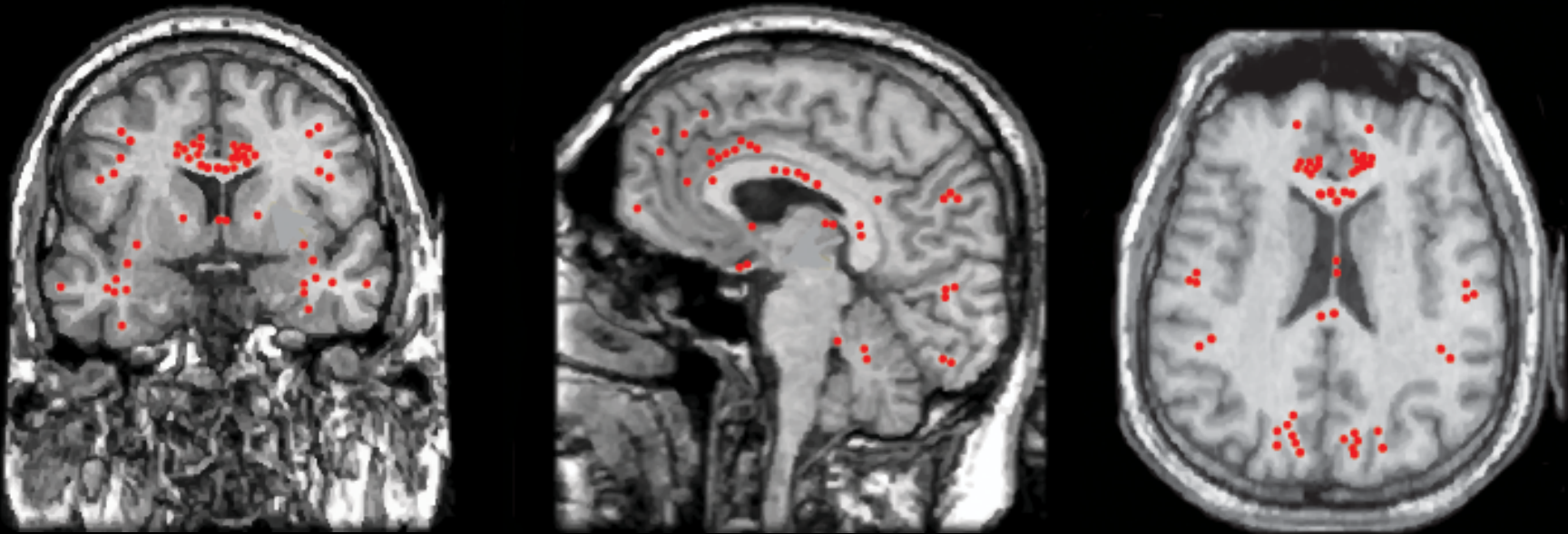
The MIND Institute

MENTAL ILLNESS AND NEUROSCIENCE DISCOVERY

- **The University of Iowa**
 - Nancy C. Andreasen, M.D. Ph.D.
 - Beng C. Ho, M.D.
 - Vincent A Magnotta, Ph. D.
 - Thomas Wassink, M.D.
- **Massachusetts General Hospital**
 - Randy Gollub, M.D., Ph.D.
 - Dara Manoach, Ph.D.
 - Don Goff, M.D.
 - Larry Siedman, Ph.D.
 - Laura Kunkel, M.D.
- **The University of Minnesota**
 - Kelvin O. Lim, M.D.
 - Bryon Mueller, Ph.D.
 - S. Charles Schulz, M.D.
 - Tonya White, M.D.
- **The University of New Mexico / MIND Institute**
 - Jeremy Bockholt
 - Juan Bustillo, M.D.
 - Vince Calhoun, Ph.D.
 - Vince Clark, Ph.D.
 - John Lauriello, M.D.

White Matter Abnormalities in Schizophrenia

Summary of 50+ Studies



White, Nelson, Lim (2009)

Authors	Methods	Results
Kumra et al. (2004)	ROI	↓ FA in <u>bilat. frontal</u> and occipital white matter regions
Kumra et al. (2005)	Voxel-based	↓ FA in L anterior cingulate region
White et al. (2007)	Voxel-based	↓ FA in L hippocampus
Kyriakopoulos et al. (2008)	Voxel-based	↓ FA in bilateral parietal association cortices and L middle cerebellar peduncle
Kendi et al. (2008)	ROI	No difference in FA in fornix but ↓ volume of the fornix
White et al. (2009)	Pothole	Greater number of potholes, more pronounced in the corpus callosum
James et al. (2011)	Voxel-based	Wide-spread reductions in FA

University of Minnesota

Patients n = 27

Controls n = 22

Massachusetts General Hospital

Patients n = 28

Controls n = 21



University of New Mexico

Patients n = 41

Controls n = 43

University of Iowa

Patients n = 19

Controls n = 52

	Patients (n = 114)		Controls (n = 138)	
	Chronic (n = 83)	First-Episode (n = 31)	Chronic Control (n = 95)	First-Episode Control (n = 43)
Age (years, SD)	36.4 (11.0)	25.2 (6.7)	34.0 (11.3)	25.2 (6.6)
Sex (M / F)	62 / 21	22 / 9	57 / 38	24 / 19
Hand (R / L / Both)	73 / 3 / 6	26 / 3 / 1	86 / 5 / 3	41 / 2 / 0
WRAT 3rd (Reading)	46.8 (6.2)	47.1 (6.6)	50.8 (4.5)	50.2 (3.9)
Father's Education	14.3 (3.3)	13.9 (4.7)	15.0 (3.7)	14.6 (2.3)
Mother's Education	13.3 (3.6)	14.1 (3.2)	13.8 (2.9)	14.1 (2.3)
BMI	28.9 (6.7)	24.9 (3.0)	26.4 (5.3)	24.1 (4.2)

Acquisition Parameters at Four sites

	Iowa	MGH	UMinn	NMex
Diffusion Tensor Images				
Scanner	Siemens 3T TRIO	Siemens 1.5 T Sonata	Siemens 3T TRIO	Siemens 1.5 T Sonata
TR (ms)	9,500	8,900	10,500	9800
TE (ms)	90	80	98	86
Voxel Dimensions (mm)	2 x 2 x 2	2 x 2 x 2	2 x 2 x 2	2 x 2 x 2
Diffusion Directions	6	60	12	12
B-Values (s/mm²)	0 / 1,000	0 / 700	0 / 1,000	0 / 1,000
NEX	4	1	2	4
Bandwidth (Hz/pixel)	1,954	1,860	1,342	1,502

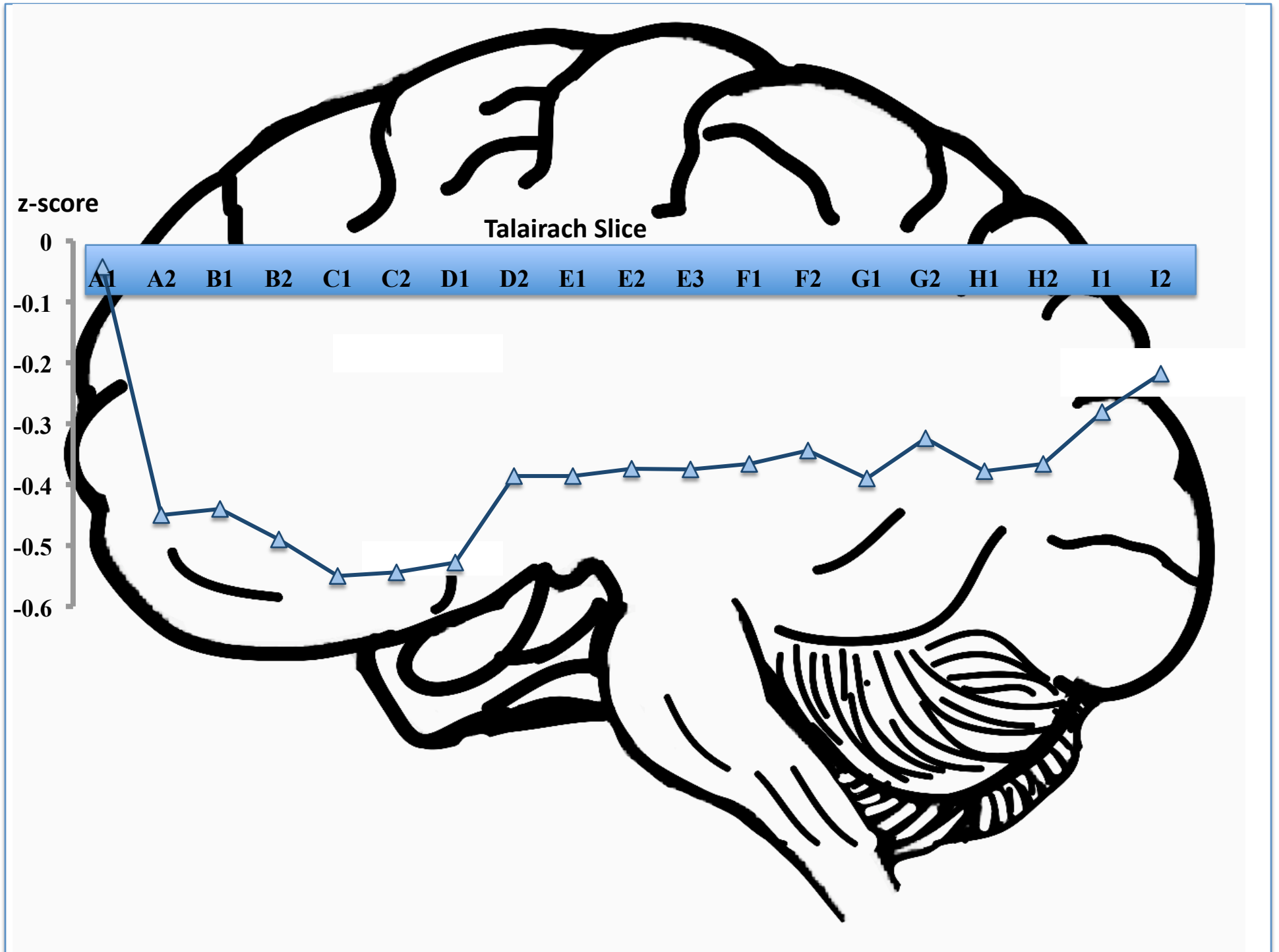
Initial Report:

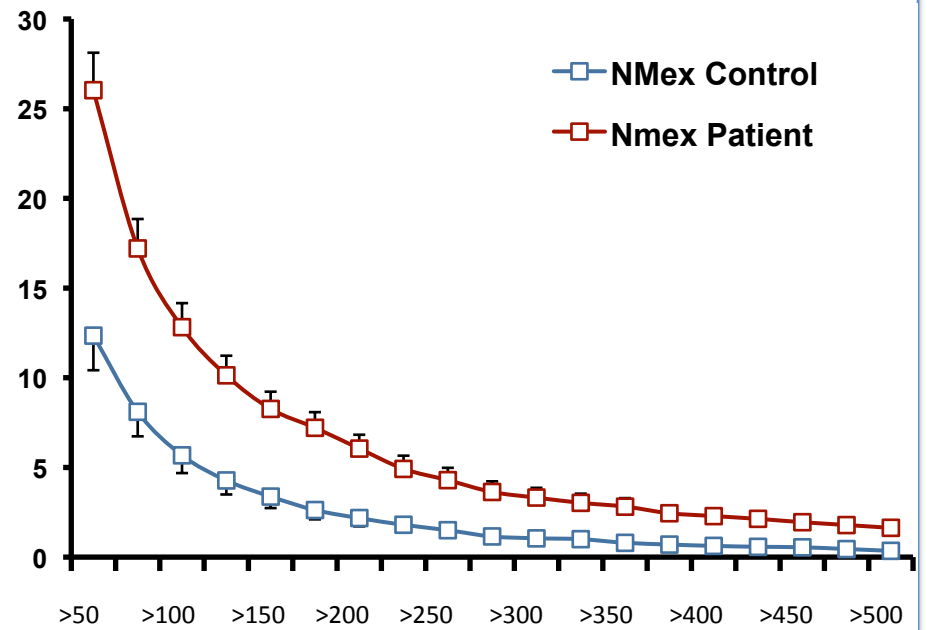
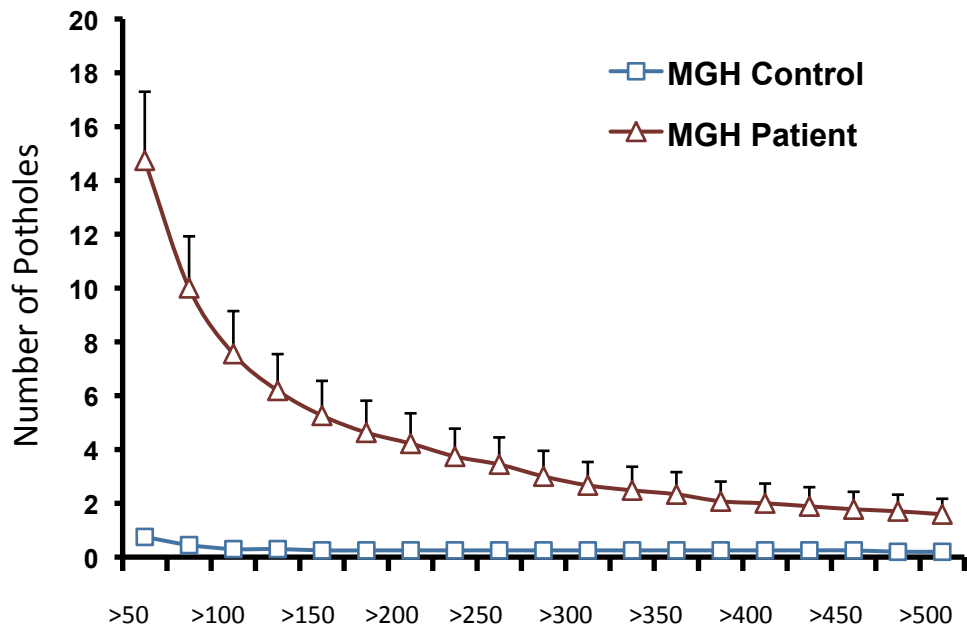
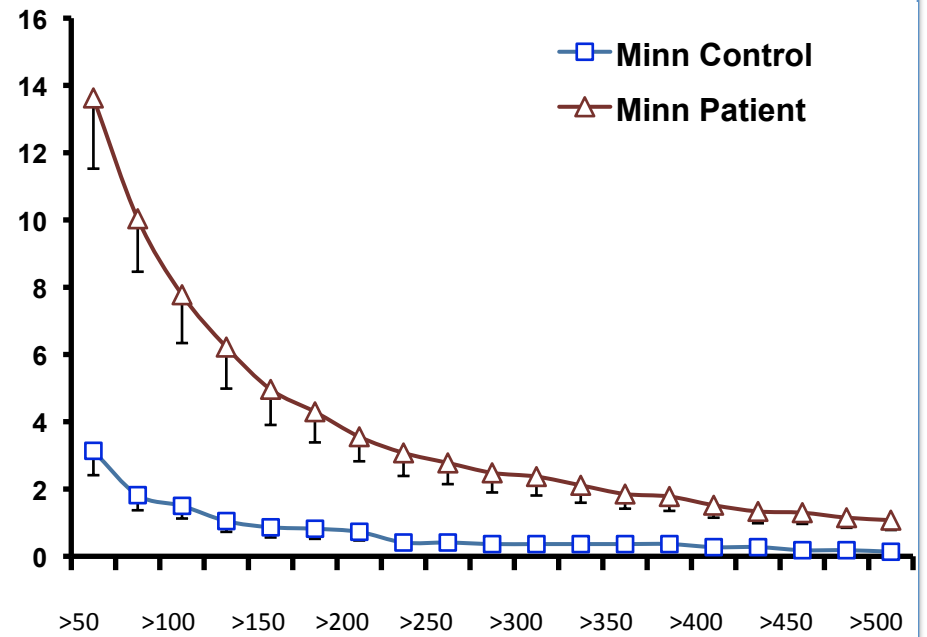
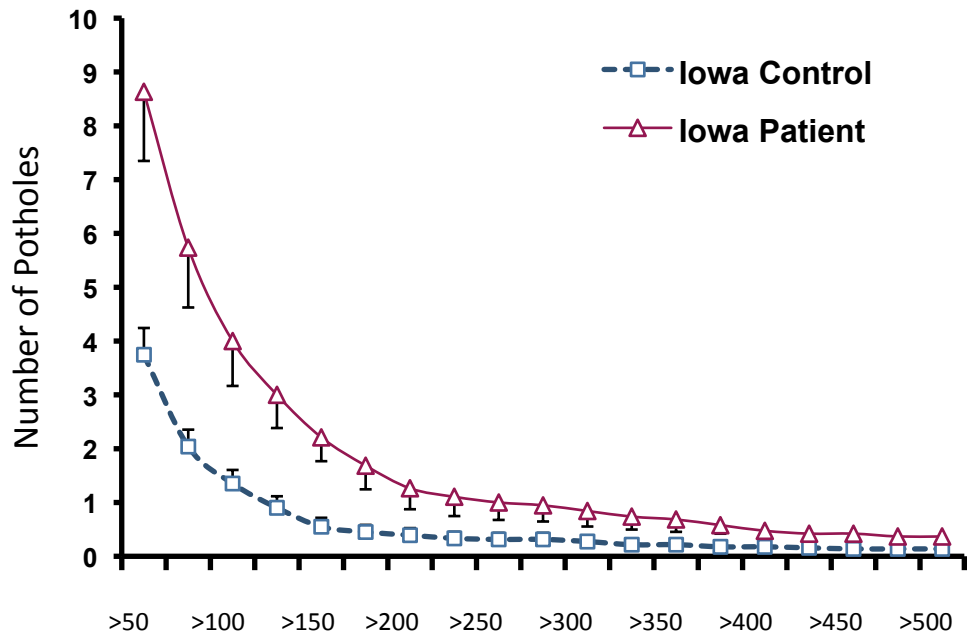
White T, Magnotta VA, Bockholt HJ, et al. Global white matter abnormalities in schizophrenia: a multisite diffusion tensor imaging study. *Schizophrenia Bulletin*. Jan 2011;37(1):222-232.

Currently under review:

Spatial Characteristics of White Matter Abnormalities in Schizophrenia

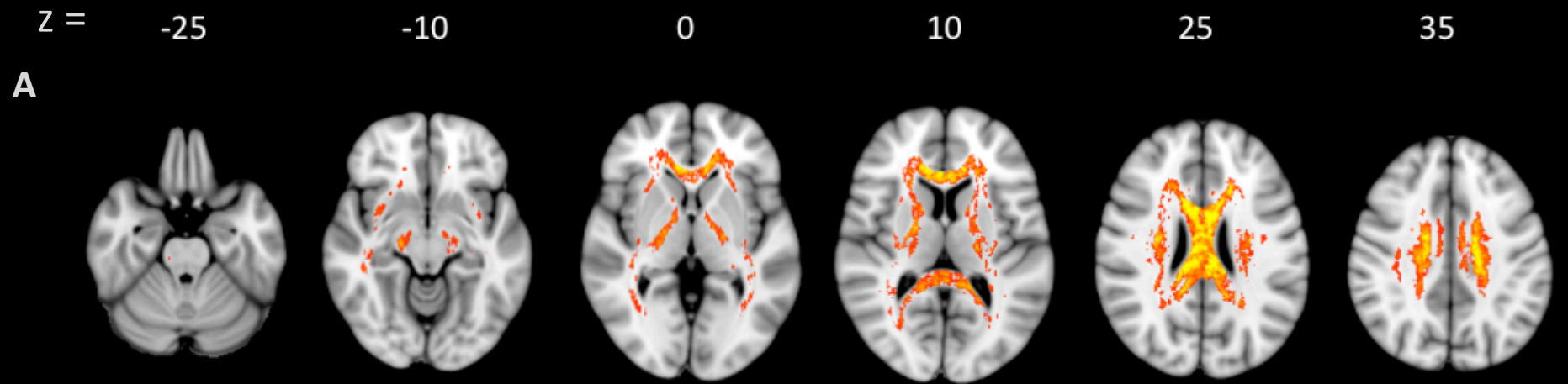
Tonya White, M.D., Ph.D.^{1,2}, H. Jeremy Bockholt^{3,4}, Stefan Ehrlich, M.D.^{5,6}, Beng C. Ho, M.D.⁷, Dara S. Manoach^{5,8}, Vincent P. Clark, Ph.D.^{4,9}, Randy L. Gollub, M.D., Ph.D.^{5,8}, Vince D. Calhoun, Ph.D.^{4,10}, S. Charles Schulz, M.D.¹¹, Nancy C. Andreasen, M.D., Ph.D.⁷, Kelvin O. Lim, M.D.¹¹, Vincent A. Magnotta, Ph.D.¹²



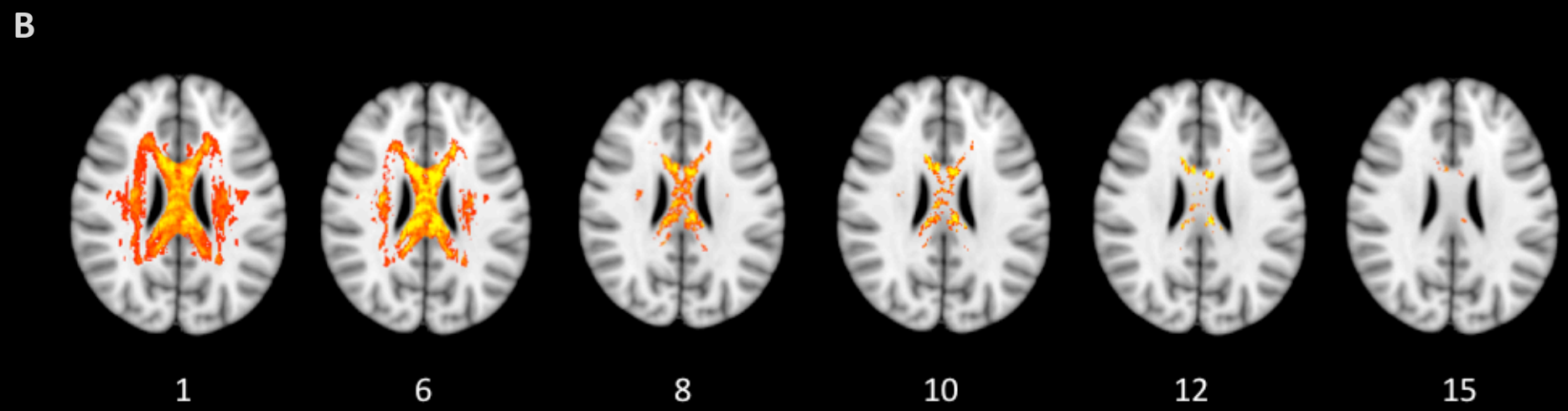


Number of Contiguous Voxels

Number of Contiguous Voxels



Spatial Location of at Least Six Overlapping Potholes in Patients



Number of Overlapping Potholes at z = -25

Conclusions

- There is considerable evidence that abnormalities in white matter play a significant role in the neuropathology of schizophrenia
- There is considerable heterogeneity in the spatial location of white matter abnormalities in schizophrenia
 - First-episode and early-onset patients have more focal abnormalities
 - It is possible that the heterogeneity in clinical symptoms parallels the heterogeneity in white matter abnormalities.